

## Mid-infrared observations of three compact HII regions and PAH emission

R. P. Verma, S. K. Ghosh, A. D. Karnik, B. Mookerjea and T. N. Rengarajan

*Tata Institute of Fundamental Research, Homi Bhabha Road, Mumbai 400005, India*

### 1. Introduction

In recent years the presence of Polycyclic Aromatic Hydrocarbon (PAH) molecules has been demonstrated in a variety of astronomical sources. In order to assess the importance of PAH emission in compact HII regions, we have observed two ultra compact HII regions (IRAS 19181+1349 and 20178+4046) and one molecular clump (IRAS 20286+4105) at mid infrared wavelengths using the ISOCAM instrument of Infrared Space Observatory (ISO)<sup>1</sup>. The imaging has been done in seven spectral bands; four of these bands cover the emission from PAH molecules; the remaining three cover the neighbouring continua and serve as comparison.

Some of the resulting images are shown in this paper. These sources have also been mapped in two far infrared bands (with effective wavelengths of  $\sim 130 \mu\text{m}$  and  $\sim 210 \mu\text{m}$ ) using TIFR 1m balloon-borne telescope. These maps cover a larger area and have a resolution of  $\sim 1'$ . Some of the far infrared maps are also shown for comparison.

### 2. Observations and results

Observations have been made using the ISOCAM instrument of ISO in single pointing mode. We have imaged an area of  $3' \times 3'$  around each source (with a pixel size of  $6''$ ) using SW as well as LW array. Seven spectral bands in which observation were made, are shown in Table 1. Adequate exposures for stabilization of detectors have been included. Raw data were

**Table 1.** Bands of Observation

| Band | $\lambda$          | Bandwidth         | Type        |
|------|--------------------|-------------------|-------------|
| SW2  | $3.3 \mu\text{m}$  | $0.2 \mu\text{m}$ | PAH feature |
| SW6  | $3.7 \mu\text{m}$  | $0.5 \mu\text{m}$ | Comparison  |
| LW4  | $6.0 \mu\text{m}$  | $1.0 \mu\text{m}$ | PAH feature |
| LW5  | $6.75 \mu\text{m}$ | $0.5 \mu\text{m}$ | Comparison  |
| LW6  | $7.7 \mu\text{m}$  | $1.5 \mu\text{m}$ | PAH feature |
| LW7  | $9.6 \mu\text{m}$  | $2.4 \mu\text{m}$ | Comparison  |
| LW8  | $11.4 \mu\text{m}$ | $1.1 \mu\text{m}$ | PAH feature |

Based on observations with ISO, an ESA project with instruments funded by ESA Member States (especially the PI countries : France, Germany, the Netherlands and the United Kindom) with the participation of ISAS and NASA.

processed at ESTEC using Auto Analysis Processing. Some of the resulting calibrated images for IRAS 19181+1349 are shown in Figure 1. In the same figure are shown maps obtained from TIFR 1m balloon-borne telescope during a flight made on February 20, 1994. These maps, at effective wavelengths of  $\sim 130 \mu\text{m}$  and  $\sim 210 \mu\text{m}$  cover larger area ( $\sim 30' \times 25'$ )

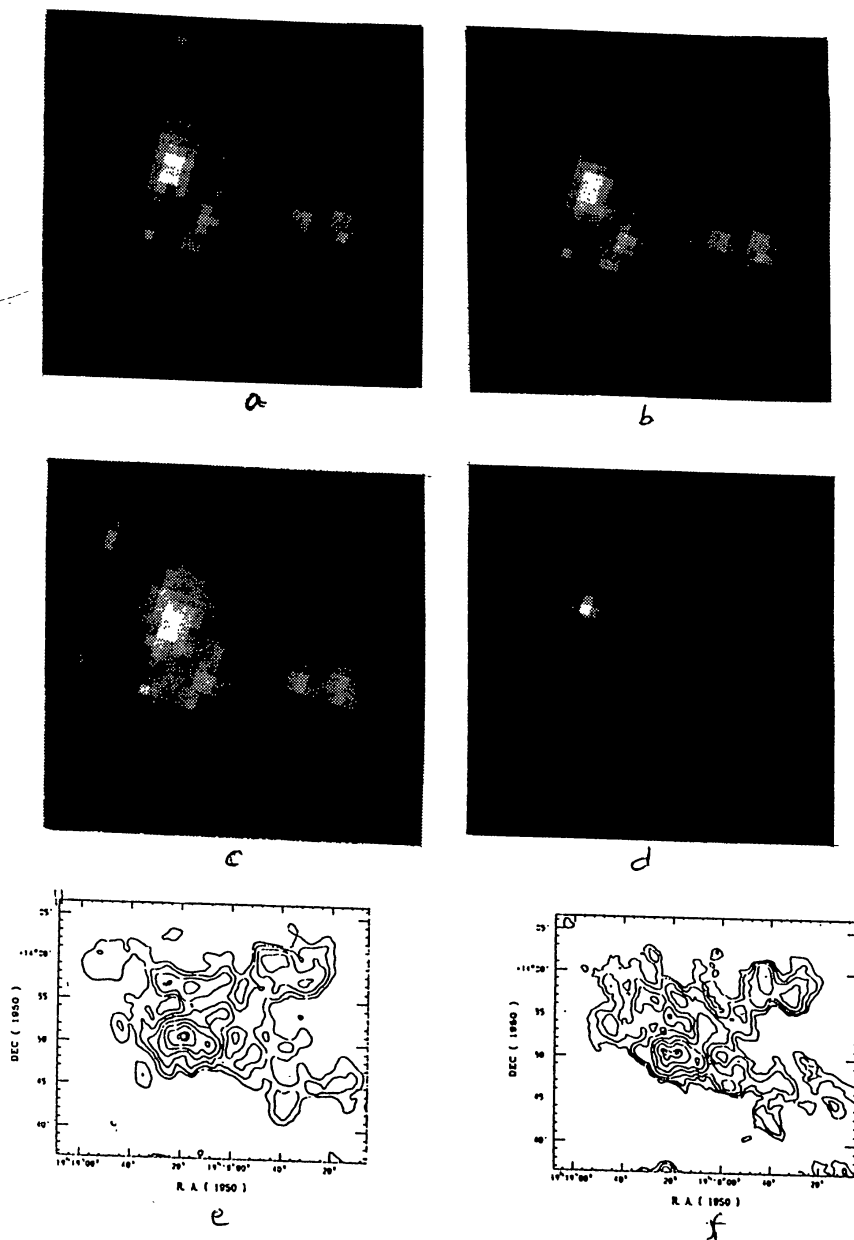


**Figure 1.** ISOCAM LW images and far infrared maps of IRAS 19181+1349. ISOCAM images are shown at a)  $6.0 \mu\text{m}$ , b)  $6.75 \mu\text{m}$ , c)  $7.7 \mu\text{m}$  and d)  $9.6 \mu\text{m}$ . Far infrared maps are shown at e)  $130 \mu\text{m}$  and f)  $210 \mu\text{m}$ . The contour levels in the far infrared maps are at 95, 80, 40, 20, 10, 5, 2.5 and 1.0 percent of the peak flux densities, which are 867 and 189 Jy/sq. arc min. at  $130 \mu\text{m}$  and  $210 \mu\text{m}$  respectively.

with a resolution of  $\sim 1'$ . It can be seen that inspite of very different wavelengths and resolutions, the two sets of maps bear striking similarity. The source has two components separated mostly in E-W direction. The two components are clearly resolved in ISO LW images as well as the far infrared map at  $210 \mu\text{m}$ ; at  $130 \mu\text{m}$  the two components are not resolved but the elongation along E-W can be seen. Similar resemblances are seen for other sources also. IRAS 20286+4105 is resolved into two components in ISO images but is unresolved in far infrared maps.

A search was made in the ISO images for point sources using a central point spread function. The positions and fitted flux densities for the strong point sources are given in Table 2. It can be seen that for all the sources, the flux densities in PAH bands are much higher than the corresponding flux densities in the neighbouring continua. This shows that for these source PAH molecules play a very important role.

**Table 2.** Observed flux densities of strong point sources in the ISO images.

| Sources<br>IRAS | RA<br>(2000) | DEC<br>(2000) | Flux Density in Jy |       |            |      |            |      |            |
|-----------------|--------------|---------------|--------------------|-------|------------|------|------------|------|------------|
|                 |              |               | SW2<br>PAH         | SW6   | LW4<br>PAH | LW5  | LW6<br>PAH | LW7  | LW8<br>PAH |
| 19181+1349      | 19 20 30.7   | +13 55 36     | 0.12               | 0.086 | 1.10       | 1.34 | 2.85       | -    | 0.32       |
| 19181+1349      | 19 20 30.4   | +13 55 46     | 0.55               | 0.56  | 1.22       | -    | 2.58       | 1.16 | 3.24       |
| 20286+4105      | 20 30 27.5   | +41 15 51     | -                  | -     | 2.75       | 1.99 | 7.47       | 2.05 | 3.76       |
| 20286+4105      | 20 30 27.2   | +41 15 21     | -                  | -     | 3.18       | 2.57 | 7.30       | 2.10 | 4.46       |
| 20178+4046      | 20 19 39.3   | +40 56 28     | -                  | -     | 10.8       | 10.3 | 28.7       | 12.2 | 22.9       |
| 20178+4046      | 20 19 38.0   | +40 56 49     | 0.86               | 0.53  | -          | -    | -          | -    | -          |

### 3. Conclusions

For all the sources, the flux densities are higher in the bands covering PAH features as compared to the neighbouring continua, thus underlining the importance of PAH molecules. There are structural similarities between the mid IR images from ISO and far infrared maps from balloon-borne telescope inspite of very different angular resolution and wavelengths.